Supporting Information for:

Designing Ultratough, Malleable and Foldable Biocomposites for Robust Green Electronic Devices

*Xunan Hou[a], Siqi Liu[a], Chaobin He[*a,b]*

[a]Department of Materials Science and Engineering, National University of Singapore, 9 Engineering Drive 1, Singapore 117575

[b]Institute of Materials Research and Engineering, Agency for Science, Technology, and Research (A*STAR), 2 Fusionopolis Way, Innovis, Singapore 138634

This file contains:

Supporting Text

Figures S1-S9

Tables S1-S5

Supporting Text

1. Theory

Dependence of glass transition on composition is a semiquantitative method to assess the attractive interaction between polymers. The Tg-composition dependence can be interpreted from the Gordon-Taylor equation[1]:

$$T_g = T_{g,1} + \frac{kw_1(T_{g,2} - T_{g,1})}{w_1 + kw_2} \quad \text{(Eq. S1)}$$

where $T_{g,i}$ are the glass transition temperatures, while w_i are the weight fractions of each component. k is an adjustable parameter related to changes in heat capacity during glass transition:

$$k = \frac{\Delta c_{p2}}{\Delta c_{p1}}(1 + w_1\frac{\partial c_p^l}{\Delta c_{p2}} + w_2\frac{\partial c_p^g}{\Delta c_{p1}}) \quad \text{(Equation S2)}$$

where Δc_{pi} denotes the change in heat capacity c_{pi} at glass transition for the ith component. c_{pi} was measured according to literature [2]. k is calculated from c_{pi} values before and after the T_g. ∂c_p^l and ∂c_p^g are the derivative change in heat capacity in the liquid and glass phase, respectively. Lu et al. [1] developed a modified Gordon-Taylor model to predict T_g-composition relationships in binary polymer blends. When interactions between the components are negligible, ∂c_p^l and ∂c_p^g become infinitesimal and the k value is reduced to $K_0 = \frac{\Delta c_{p2}}{\Delta c_{p1}}$.

2. Differential scanning calorimetry (DSC)

In the LBO composites, the determination of T_g of PLA and PHB phase is not reliable due to: i) The endothermic peak of the PHB rigid amorphous fractions[3,4] overlapping with the T_g of

PLA phase (40-55 °C); ii) the high crystallinity of PHB that hinders occurring near its T_g (-5 to 5 °C).

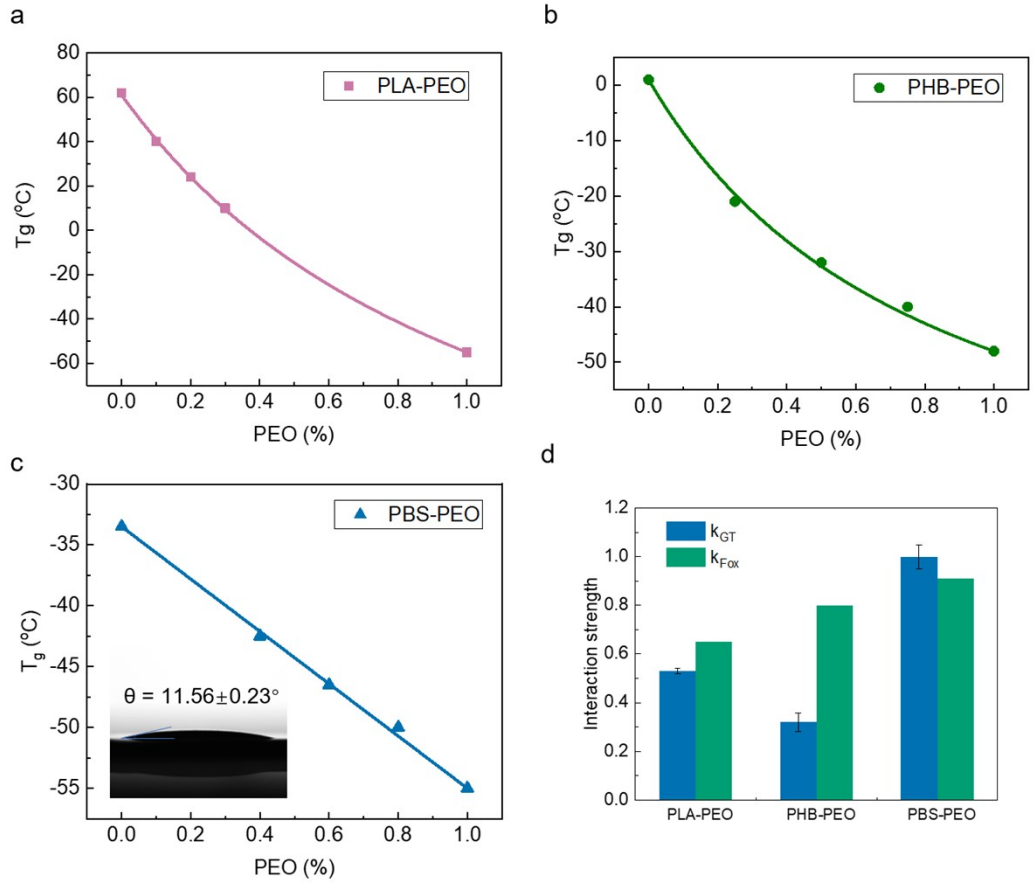

Fig. S1 (a-c) Glass transition temperature – composition relationship in binary biodegradable polymer blends. (d) interaction strength parameter k_{GT} and critical value k_{Fox} of three polymer pairs.

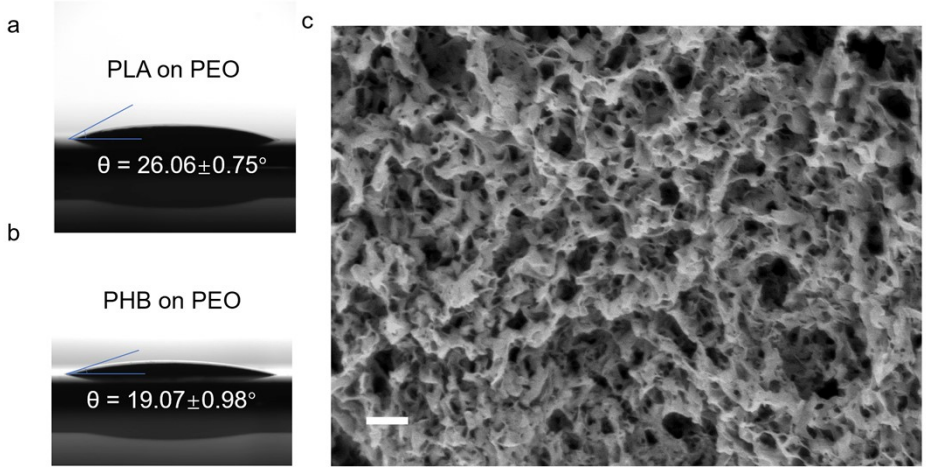

Fig. S2 (a-b) melt contact angle between polymers. (c) FESEM images of cryo-impact surface after solvent etching. Scale bar is 2 μm.

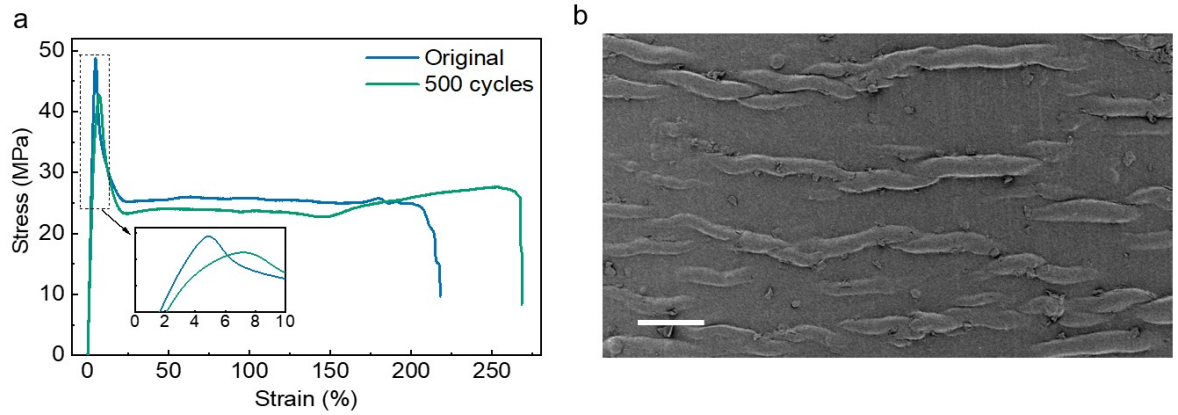

Fig. S3 (a) Stress-strain curves of LBO-3 blends (~3mm thick) after 500 cycles of 180° bend. (b) SEM images of the LBO-3 blend. Scale bar is 100 μm.

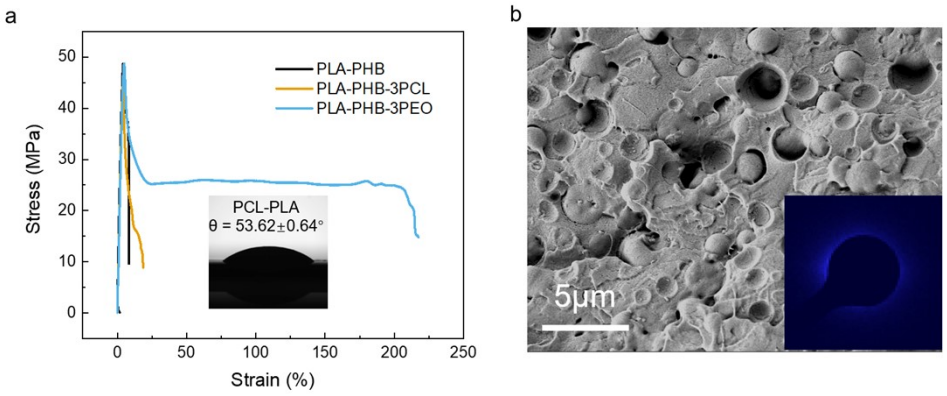

Fig. S4 (a) Stress-strain curves of different polymer systems compared with PLA-PHB-PEO blends. Inset: contact angles of relevant polymer pairs. (b) FESEM images of tensile fractured surface of PLA-PHB-3PCL. Inset: corresponding SAXS patterns. Color scale: 0-2000.

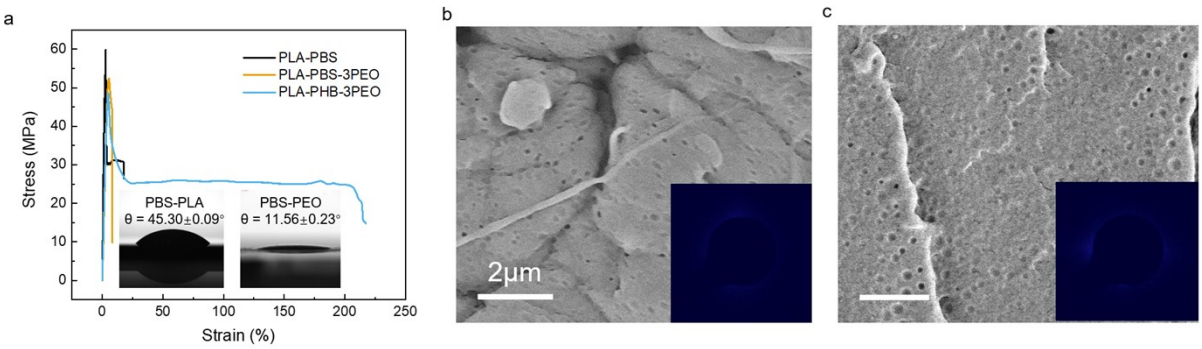

Fig. S5 (a) Stress-strain curves of different polymer systems compared with PLA-PHB-PEO blends. Inset: contact angles of relevant polymer pairs. FESEM images of tensile fractured surfaces of (b) PLA-PBS (c) PLA-PBS-3PEO. Inset: corresponding SAXS patterns. Color scale: 0-2000.

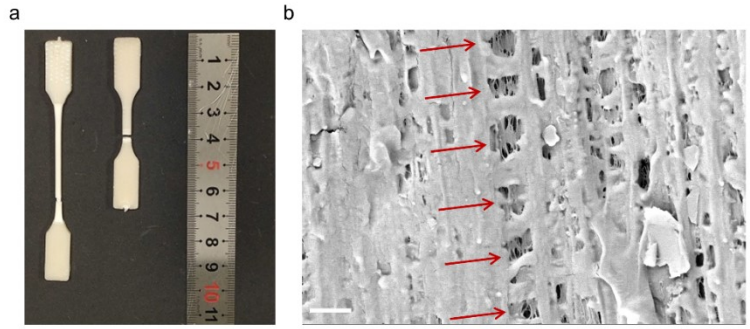

Fig. S6 (a) Digital images showing the tensile elongation in LBO-3 (left) compared to LBO-0 (right); (b) SEM images showing crazes in fractured LBO-3 sample. Tension direction is near vertical.

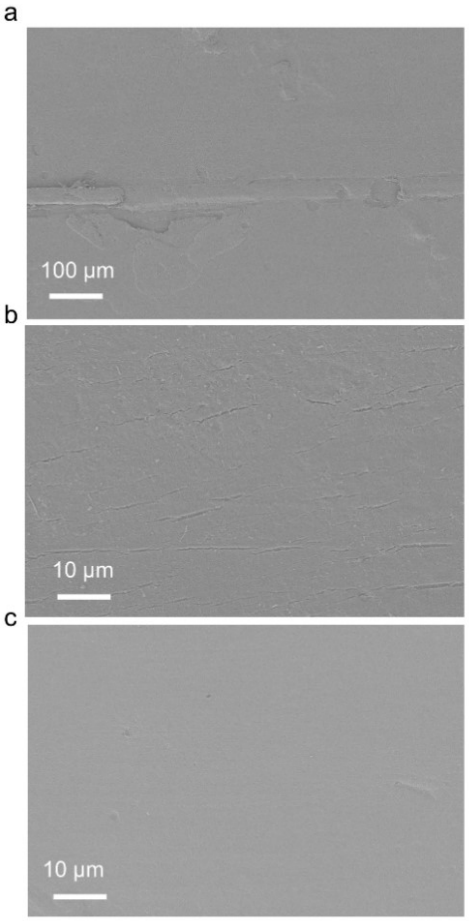

Fig. S7 SEM images of 50 µm thick films of (a) (b) neat PLA after 10 cycle 90^{o} folds; (c) LBO-3 sample after 500 cycle 90^{o} fold.

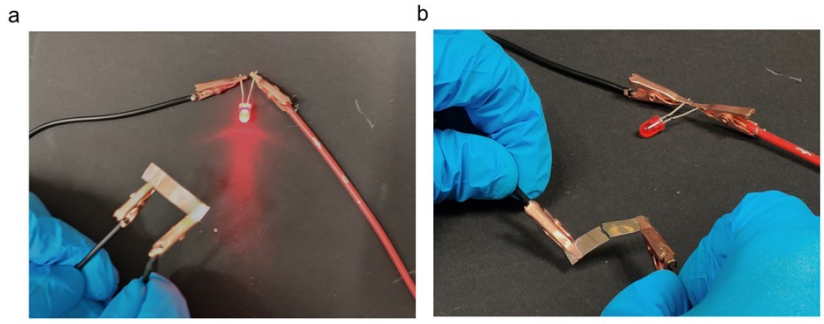

Fig. S8 Electronic conduction test of LBO-0 film: (a) original form; (b) bent and fractured with open-circuit.

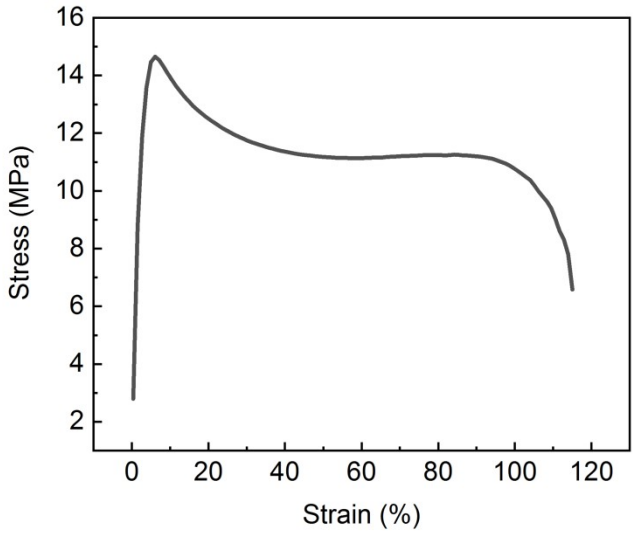

Fig. S9 Representative stress-strain curve of crumpled LBO-3 film up to >100% elongation. The lower tensile strength was due to different processing pressures for thin films (~20 MPa) and bulk samples (~70 MPa)

Table S1 Mechanical properties of polymer blends and ternary biocomposites, along with standard deviations (σ)

	Modulus	σ	Strength	σ	Elongation	σ	Toughness[1]	σ
	[GPa]	[GPa]	MPa	MPa	[%]	[%]	[MJ/m^3]	[MJ/m^3]
PLA	3.44	0.25	64.12	0.75	3.65	0.85	1.15	0.24
PHB	0.59	0.08	12.38	0.27	2.97	0.21	0.23	0.05
LBO-0[2]	3.37	0.22	48.09	0.54	5.79	2.24	1.74	0.95
LBO-3	3.45	0.15	49.27	0.51	247.93	26.66	62.84	6.09
LBO-5	2.76	0.12	47.83	0.94	300.23	13.91	86.58	7.54
BO-1	0.55	0.03	13.52	0.47	5.73	1.13	0.46	0.07
BO-3	0.53	0.02	13.72	0.42	8.39	1.45	0.59	0.06
BO-5	0.52	0.02	13.00	0.38	8.25	0.96	0.74	0.10
LBO-10	1.72	0.16	23.64	1.92	207.56	14.41	44.56	1.24
LBC-3	3.25	0.14	44.26	0.57	16.10	2.35	2.40	0.38
LS-25	3.56	0.27	58.01	0.87	161.50	18.15	53.18	5.23
LSO-3	3.45	0.32	51.67	0.72	10.23	1.24	3.50	0.47

[1]: calculated from the area under stress-strain curves.

[2]: Abbreviated forms: L = PLA, B = PHB, O = PEO, C = PCL, S = PBS; For ternary composites, 1st component is the continuous phase, the 2nd component is the disperse phase (fixed at 25% wt).

Table S2 Parameters from statistical analysis of FESEM images (ImageJ software).

Slice	Count	Total Area	Average Size	Feret	MinFeret
	-	nm^2	nm^2	nm	nm
LBO-0	22	37845983	1720271.955	1716.178	1361.23
LBO-3	77	4608025	59844.477	299.963	217.402

Table S3

Comparison of the mechanical properties of LBO blends with literature reports of other polymer blends/ composites.

Parameters	Strength	Elongation	Toughness*	Reference
Units	MPa	%	MJ/m^3	
PS/PPE (Noryl®)	35-68	25-82	17-28.7	[5]
ABS/PC	45-50	40-80	18-40	[5]
PP/elastomer (TPV)	6.2-8.8	45-100	19-43.12	[5]
PHB/PHBV	22.6-25.6	539-589	99.8-103.5	[6]
PLA/EB	22-40	130-220	28-40	[7]
PE/iPP	20-25	180-400	36-88	[8]
Ag/Au/SBS	3-22	180-840	4.5-93.5	[9]
PVA/GO	64-120	1.2-2.4	1.44-1.53	[10]
PLA/CSNP	33-35	48-288	14-75	[11]
UHMWPE/GO	23-27	75-290	17.25-78.3	[12]
PLA/PoSS	38-52	48-65	18.2-29.2	[13]
PVAm/PVA	20-70	16-40	8-22	[14]
PLA/PHB/PEO	47-50	198-301	60-85	This work

*Values are determined from the area below the stress-strain curves, or estimated from strength and elongation values

Table S4 Thermal properties of LBO-x ternary biocomposites

	T_{α}[a]	$T_{cc,PLA}$[b]	$T_{m,PLA}$[b]	$T_{m,PHB}$[b]	$\Delta H_{cc,PLA}$[c]	$\Delta H_{m,PLA}$[c]	$\Delta H_{m,PHB}$[c]	$X_{c,PLA}$[d]	$X_{c,PHB}$[d]
	°C	°C	°C	°C	J/g	J/g	J/g	%	%
LBO-0	57.41	100.49	154.20	172.42	26.15	27.32	14.25	1.68	39.04
LBO-3	52.51	87.13	153.78	169.47	21.50	23.37	14.43	2.79	39.53
LBO-5	51.94	81.64	153.03	168.96	23.33	25.15	15.16	2.80	41.53
LBO-10	51.53	88.57	153.61	167.96 175.04	16.01	19.71	14.57	6.12	39.92

a) Weight percentage of PMMA. b) glass-rubbery transition temperature from DMA tand curve. c) Obtained from DSC thermogram: the glass transition temperature (T_g), cold crystallization temperature (T_{cc}), enthalpy of cold crystallization (ΔH_{cc}) and melting (ΔH_m). d) calculated using the formula $X_c = \frac{\Delta H_{m,i} - \Delta H_{cc,i}}{w_i \Delta H_{c,i}}$, where w is the weight fraction of the polymer in the blend, $\Delta H_{c,i}$ is the crystallization enthalpy of fully crystallized polymer. $\Delta H_{c,PLA} = 93$ J/g[15], $\Delta H_{c,PHB} = 146$ J/g[16].

Table S5 TGA results of binary and ternary blends

	$T_{d,onset,\ PHB}$ °C	$T_{max,\ PHB}$ °C	$T_{max,\ PLA}$ °C	T_{50} °C
LBO-0	248.04	266.93	353.83	333.36
LBO-3	267.67	284.33	355.47	345.52
LBO-5	280.21	292.90	362.12	346.65

References

[1] X. Lu, R. A. Weiss, *Macromolecules* **1992**, *25*, 3242.

[2] American Society for Testing and Materials (ASTM®), *ASTM Stand.* **2011**, *i*, 1.

[3] M. L. Di Lorenzo, M. C. Righetti, *J. Therm. Anal. Calorim.* **2013**, *112*, 1439.

[4] M. L. Di Lorenzo, M. Gazzano, M. C. Righetti, *Macromolecules* **2012**, *45*, 5684.

[5] L. A. Utracki, C. A. Wilkie, *Polymer Blends Handbook* (Eds.: Utracki, L. A.; Wilkie, C. A.), Springer Netherlands, Dordrecht, **2014**.

[6] X. Tang, A. H. Westlie, E. M. Watson, E. Y. X. Chen, *Science (80-.).* **2019**, *366*, 754.

[7] R. Li, L. Wu, B. G. Li, *Eur. Polym. J.* **2018**, *100*, 178.

[8] J. M. Eagan, J. Xu, R. Di Girolamo, C. M. Thurber, C. W. Macosko, A. M. La Pointe, F. S. Bates, G. W. Coates, *Science (80-.).* **2017**, *355*, 814.

[9] S. Choi, S. I. Han, D. Jung, H. J. Hwang, C. Lim, S. Bae, O. K. Park, C. M. Tschabrunn, M. Lee, S. Y. Bae, J. W. Yu, J. H. Ryu, S. W. Lee, K. Park, P. M. Kang, W. B. Lee, R. Nezafat, T. Hyeon, D. H. Kim, *Nat. Nanotechnol.* **2018**, *13*, 1048.

[10] Y. Q. Li, T. Yu, T. Y. Yang, L. X. Zheng, K. Liao, *Adv. Mater.* **2012**, *24*, 3426.

[11] H. He, Z. Duan, Z. Wang, *Compos. Part A Appl. Sci. Manuf.* **2020**, *128*, 105676.

[12] Y. Chen, Y. Qi, Z. Tai, X. Yan, F. Zhu, Q. Xue, *Eur. Polym. J.* **2012**, *48*, 1026.

[13] Z. Liu, D. Hu, L. Huang, W. Li, J. Tian, L. Lu, C. Zhou, *Chem. Eng. J.* **2018**, *346*, 649.

[14] A. Eckert, T. Rudolph, J. Guo, T. Mang, A. Walther, *Adv. Mater.* **2018**, *30*, 1.

[15] S. Saeidlou, M. A. Huneault, H. Li, C. B. Park, *Prog. Polym. Sci.* **2012**, *37*, 1657.

[16] P. J. Barham, A. Keller, E. L. Otun, P. A. Holmes, *J. Mater. Sci.* **1984**, *19*.